Mitochondrial activity as an indicator of fish freshness

Jérôme Cleach, Philippe Pasdois, Philippe Marchetti, Denis Watier, Guillaume Duflos, Emmanuelle Goffier, Anne-Sophie Lacoste, Christian Slomianny, Thierry Grard, Philippe Lencel

Mitochondrial activity as an indicator of fish freshness

Jérôme Cléach[a,b,c,d,e], Philippe Pasdois[f], Philippe Marchetti[g], Denis Watier[a], Guillaume Duflos[h], Emmanuelle Goffier[i], Anne-Sophie Lacoste[j], Christian Slomianny[k], Thierry Grard[a§*] and Philippe Lencel[a§]

[a] *Univ. Littoral Côte d'Opale, USC ANSES, EA 7394 – ICV – Institut Charles Viollette, F-62200 Boulogne-sur-Mer, France*

[b] *Univ. Lille, F-59000 Lille, France*

[c] *Univ. Artois, F-62000 Arras, France*

[d] *INRA, French National Institute for Agricultural Research*

[e] *ISA, F-59000 Lille, France*

[f] *Univ. Bordeaux, INSERM U1045, IHU-LIRYC, F-33600 Pessac, France*

[g] *Univ. Lille, INSERM UMR S1172, Jean Pierre Aubert Research Centre, F-59045 Lille, France*

[h] *ANSES, Laboratoire de Sécurité des Aliments, Boulevard du Bassin Napoléon, F-62200 Boulogne-sur-Mer, France*

[i] *PFINV, F-62200 Boulogne-sur-Mer, France*

[j] *Univ. Lille, Bio Imaging Center Lille, Lille, F-59000, France*

[k] *Univ. Lille, INSERM U.1003, Laboratoire de Physiologie Cellulaire, F- 59650, Villeneuve d'Ascq, France*

[§]T. Grard and P. Lencel share co-authorship of this article.

[*]Corresponding author: Thierry Grard

Tel: +33 3 21 99 25 08. E-mail address: thierry.grard@univ-littoral.fr

Declarations of interest: none

Abstract

The current methods used to routinely assess freshness in the fishing industry reflect more a state of spoilage than a state of freshness. Mitochondria, the seat of cellular respiration, undergo profound changes in *post mortem* tissues. The objective of this study was to demonstrate that mitochondrial activity constitutes a putative early fish freshness marker. The structure of gilthead sea bream (*Sparus aurata*) muscle tissue was evaluated over time by transmission electron microscopy. Respiration was assessed in mitochondria isolated from sea bream fillets using oxygraphy. Membrane potential ($\Delta\Psi_m$) was determined by fluorescence (Rhodamine 123). Mitochondrial activity of fillets stored at +4°C was studied for 6 days. Changes in mitochondrial cristae structure appeared from Day 3 highlighting the presence of dense granules. $\Delta\Psi_m$ and mitochondrial activity were significantly disrupted in sea bream fillets after 96 hours of storage at +4°C. Mitochondrial activity constituted a reliable and early indicator of fish freshness.

Chemical compounds used in this study:

- Rhodamine 123 (PubChem CID: 9929799)
- Carbonyl cyanide 3-chlorophenylhydrazone (PubChem CID: 2603)
- Tris (hydroxymethyl)aminomethane (PubChem CID: 6503)
- Ethylene-bis(oxyethylenenitrilo)tetraacetic acid (PubChem CID: 6207)
- 4-Morpholinepropanesulfonic acid (PubChem CID: 70807)
- Malate (PubChem CID: 525)
- Succinate (PubChem CID 160419)
- Glutamate (PubChem CID: 33032)
- Adenosine 5′-diphosphate (PubChem CID: 128882)
- Carboxyatractyloside (PubChem CID: 20055804)

- Cytochrome c (PubChem CID 16057918)
- Potassium chloride (PubChem CID: 4873)
- Sucrose (PubChem CID: 5988)
- Magnesium chloride (PubChem CID: 5360315)
- Potassium dihydrogen phosphate (PubChem CID: 516951)
- Dimethyl sulfoxide (PubChem CID: 679)
- Glutaraldehyde (PubChem CID: 3485)
- Sodium cacodylate (PubChem CID: 2724247)
- Osmium tetroxide (PubChem CID: 30318)
- Uranyl acetate (PubChem CID: 10915)
- Acetonitrile (PubChem CID: 6342)

Keywords

Mitochondrial membrane potential (ΔΨm); mitochondrial respiration; fish freshness; gilthead sea bream (*Sparus aurata*)

1. Introduction

The quality of aquatic products is defined by objective criteria such as food safety, nutritional quality, origin, and traceability of the products (G Olafsdottir, Martinsdóttir, Oehlenschläger, Dalgaard, Jensen, Undeland, et al., 1997; G. Olafsdottir, Nesvadba, Di Natale, Careche, Oehlenschläger, Tryggvadóttir, et al., 2004). It also depends on less objective criteria such as the organoleptic properties and the freshness of the products. Fish freshness is "dependent on different biological and processing factors" (Gudrun Olafsdottir, Nesvadba, Di Natale, Careche, Oehlenschläger, Tryggvadottir, et al., 2004). To meet expectations in terms of freshness, the fishing industry is trying to improve information on the date of capture of the product. However, treatments and storage conditions can vary greatly, strongly affecting quality and fish freshness. Seafood

products are highly perishable and processing factors determine the quality of the product (Cheng, Sun, Han, & Zeng, 2014; Mendes, 2018).

Consumers are becoming more attentive and demanding concerning the quality of food, including seafood. By definition, a fish can be considered fresh when its organoleptic, physical and chemical characteristics are very close to those of a living fish (Oehlenschläger & Sörensen, 1997). Savvy consumers or experts are able to discriminate fresh products by a sensory approach. Sensory evaluation grids have been developed to train a less experienced audience. However, these approaches remain highly dependent on the consumer's level of perception and knowledge of the product.

Further research is required to develop methods to evaluate fish freshness, and there are still many challenges. Microbiological, organoleptic and chemical methods are used routinely in the fishing industry to evaluate fish freshness. As an example, the total volatile base nitrogen (TVB-N) level increases significantly during the late stages of storage (10-20 days of storage), and is therefore a limited freshness indicator (Castro, Padrón, Cansino, Velázquez, & Larriva, 2006; Parlapani, Mallouchos, Haroutounian, & Boziaris, 2014), but should rather be seen as an advanced spoilage indicator. Moreover, TVB-N/total biogenic amines (TBA) analyses are not applicable to all fish species. Therefore, research in this area and the development of new fish freshness indicators are still a challenge for scientists and industry.

Many studies have shown *post mortem* structural changes in myofibrillar proteins (Delbarre-Ladrat, Chéret, Taylor, & Verrez-Bagnis, 2006). These changes in muscle tissue have often been correlated with the mechanical properties of the tissues (texture, elasticity, suppleness, hardness, cohesion, etc.) (Taylor, Fjaera, & Skjervold, 2002). The level of myofibrillar protein degradation can be correlated with fish alteration. In some of these studies, the structural changes in myofibrillar proteins have been associated with

structural changes in *post mortem* mitochondria (María Dolores Ayala, Abdel, Santaella, Martínez, Periago, Gil, et al., 2010; Parsons & Green, 2010). Studies using electron microscopy have reported *post mortem* morphological mitochondrial changes such as swelling and disrupted cristae in muscle in cold storage from the gilthead sea bream (*Sparus aurata*) (María Dolores Ayala, et al., 2010) and the Pacific bluefin tuna (*Thunnus orientalis*) (Roy, Ando, Itoh, & Tsukamasa, 2012). We focused on mitochondria to study their structural and functional changes in sea bream fillets stored at +4°C.

Mitochondria play a central role in cell death mechanisms such as apoptosis and necrosis (Parsons & Green, 2010). Several studies have shown that mitochondrial activity was still present *post mortem* in storage conditions of +4°C in bovine, murine and human models (Barksdale, Perez-Costas, Gandy, Melendez-Ferro, Roberts, & Bijur, 2010; Cheah & Cheah, 1971; Tang, Faustman, Hoagland, Mancini, Seyfert, & Hunt, 2005). Mitochondrial activity in fish has been studied in the areas of eco-physiology (Blier & Guderley, 1993; Hilton, Clements, & Hickey, 2010; Lionetti, Mollica, Donizzetti, Gifuni, Sica, Pignalosa, et al., 2014) and eco-toxicology (Cambier, Benard, Mesmer-Dudons, Gonzalez, Rossignol, Brethes, et al., 2009; Soares, Gutierrez-Merino, & Aureliano, 2007; Van den Thillart & Modderkolk, 1978). However, to our knowledge, there are currently no studies on the impact of storage at +4°C on *post mortem* changes in fish mitochondrial structure and function.

The purpose of this study was therefore to evaluate whether mitochondrial structure and function could be considered reliable and early markers of fish freshness.

To determine *post mortem* changes in mitochondrial structure and function, two approaches were used: firstly, morphological changes were analysed by transmission electron microscopy; and secondly, a functional analysis was performed to assess the

oxygen consumption and membrane potential ($\Delta\Psi_m$) of mitochondria isolated from gilthead sea bream fillets stored at +4°C.

2. Materials and methods

2.1 Reagents and materials

Rhodamine 123 (Rh123), carbonyl cyanide 3-chlorophenylhydrazone (CCCP), Tris (hydroxymethyl)aminomethane (Trizma® base), ethylene-bis(oxyethylenenitrilo)tetraacetic acid (EGTA), proteinase type XXIV, bovine serum albumin (BSA), 4-morpholinepropanesulfonic acid (MOPS), malate, succinate, adenosine 5′-diphosphate (ADP), carboxyatractyloside (CAT) and cytochrome c from equine heart were purchased from Sigma-Aldrich (St. Louis, MO, USA). Potassium chloride (KCl) and glutamate were acquired from Fisher Labosi (Paris, France). Sucrose, magnesium chloride ($MgCl_2$), and potassium dihydrogen phosphate (KH_2PO_4) were purchased from Acros Organics (Morris, NJ, USA). Rh123 and CCCP were prepared in dimethyl sulfoxide (DMSO) purchased from Thermo Scientific (San Diego, CA, USA).

2.2 Fish muscle origin and storage

The gilthead sea bream (300-400 g) were sourced from Aquanord sea farm (Gravelines, France). This farmed fish model was chosen in order to obtain accurate data on living conditions, slaughter, and storage, which influence the study of freshness. Breeding conditions were: temperature 18 ± 6°C, pH 8.2, total ammonia < 30 pmol/L, and dissolved oxygen 99 % (v/v) to saturation (7 ppm). Within the Aquanord sea farm, the fish were killed by asphyxiation/hypothermia and kept on ice (0 to 2°C) in expanded polystyrene boxes for 4 hours of transport. We bought the fish from the company after their death. Upon arrival at the laboratory, the fish were immediately skinned and filleted. The fillets were stored on ice in a cold room (+4°C) for 5 days and used for experiments every 24 hours over 6 days: Day 0,

147 Day 1, Day 2, Day 3, Day 4 and Day 6. The ice was renewed every day. Plastic wrapping was
148 used to avoid contact between the fillets and the ice or the accumulated water.

149 *2.3. Sample preparation and transmission electron microscopy*

150 To prepare samples, as previously described (Michalec, Holzner, Barras, Lacoste, Brunet,
151 Lee, et al., 2017), 3 mm^3 pieces of muscle were cut from fillets and fixed in 2.5%
152 glutaraldehyde (Merck KGaA, Darmstadt, Germany) buffered with 0.1M sodium cacodylate
153 (Sigma-Aldrich), postfixed in 1% osmium tetroxide (Sigma-Aldrich) in the same buffer and
154 "en bloc" stained with 2% uranyl acetate (Agar Scientific, Stansted, Essex, UK). After
155 acetonitrile dehydration (Sigma-Aldrich), samples were embedded in epon-like resin (Embed-
156 812). Ultrathin sections (90 nm) were cut using a Leica UC7 ultra-microtome and collected
157 on 150 mesh hexagonal barred copper grids. After staining with 2% uranyl acetate prepared in
158 50% ethanol (Fisher, Loughborough, Leicester, UK) and incubation with a lead citrate
159 solution, sections were observed on a Hitachi H-600 transmission electron microscope
160 equipped with a W electron source (operated at 75kV) and a side mounted Hamamatsu
161 C4742-95 digital camera.

162 *2.4. Mitochondrial isolation from fish fillets*

163 The method for mitochondrial isolation was adapted from Pasdois, Parker, Griffiths, and
164 Halestrap (2011). All the steps in mitochondrial isolation were performed in a cold room at
165 +4°C. Red muscle was dissected from the fillet (10 g) and finely diced with scissors. The fine
166 pieces obtained (2-3 mm^3) were incubated at +4°C for 7 minutes under stirring in 20 mL of
167 isolation buffer (180 mM KCl, 80 mM sucrose, 5 mM $MgCl_2$, 10 mM Tris, 2 mM EGTA, pH
168 7.2 at +4°C) supplemented with 0.1 mg/mL of bacterial proteinase type XXIV. The resulting
169 tissue suspension was poured into a 30 mL glass Potter homogeniser and homogenised for 3
170 min using a motorised Teflon pestle at 300 rpm. The homogenate was centrifuged at 7 500 *g*

for 10 minutes. The resulting pellet was first washed and then resuspended in 20 mL isolation buffer containing 2 mg/mL of fatty acid free BSA and homogenised for 3 minutes at 150 rpm. The homogenate was then centrifuged at 700 *g* for 10 min. The supernatant was centrifuged at 1500 *g* for 10 min. The resulting supernatant was centrifuged again at 7 000 *g* for 10 min. The mitochondrial pellet obtained was resuspended with a low volume (50 µL) of isolation buffer in order to obtain a concentrated mitochondrial suspension. The protein concentration was determined using a Bio-Rad protein assay kit, derived from the Bradford method (1976), using BSA as a standard. Mitochondria were kept on ice at a final concentration of 60-100 mg/mL for not more than 4 h.

2.5. Measurement of mitochondrial $\Delta\Psi_m$

A Xenius XC spectrofluorometer (SAFAS, Monaco) was used to monitor the fluorescence of Rh123 (Emaus, Grunwald, & Lemasters, 1986) in order to evaluate changes in mitochondrial $\Delta\Psi_m$ of isolated mitochondria extracted at different storage times (Day 0, Day 1, Day 2, Day 3 and Day 4). Importantly, this experimental approach does not enable the user to measure $\Delta\Psi_m$ but gives a qualitative index of mitochondrial polarisation. 1 mL of respiration buffer (KCl 125 mM, MOPS 20 mM, Tris 10 mM, EGTA 10 µM, KH_2PO_4 2.5 mM, fatty acid free BSA 2 mg/mL, pH 7.2) at 25°C was added to a 3 mL plastic cuvette. Rh123 (50 nM final) and respiratory substrates – glutamate (5 mM), malate (2 mM) and succinate (5 mM) – were added sequentially. The baseline fluorescence of free Rh123 was recorded during 2 minutes and mitochondria (0.2 mg/mL) were then added. The generation of $\Delta\Psi_m$ leads to accumulation of Rh123 in the mitochondrial matrix and consequent fluorescence quenching (dye stacking). To evaluate mitochondrial function, the following additions were performed sequentially. ADP (1 mM), CAT (5 µM) and CCCP (2 µM). The sampling rate was 1 Hz, bandwidth 15 nm at excitation and emission, and photomultiplier tube voltage was 700 V. Samples were excited at 500 nm and fluorescence was collected at 535 nm.

196 The Rh123 fluorescence intensities recorded at different states of respiration (basal (substrates
197 only), state 3 (ADP addition), and CAT) were normalised to the fluorescence recorded after
198 CCCP addition, according to the following formula:

199 $$100 - \left(\left(\frac{X - Y}{X}\right) \text{x } 100\right)$$

200 Where: X = Rh123 fluorescence intensity after CCCP addition

201 Y = Rh123 fluorescence intensity after mitochondria or ADP or CAT addition

202 CCCP at 2 µM completely depolarised mitochondria by consuming all the proton gradient
203 established by the respiratory chain. Thus, the fluorescence intensity obtained after its
204 addition corresponded only to the dissipation of $\Delta\Psi_m$ and enabled us to take into account the
205 non-specific binding of the dye.

206 *2.6. Respiration assay*

207 Oxygraphy (Rank Brothers digital model 10, Cambridge, United Kingdom) was used to
208 monitor the oxygen consumption of isolated mitochondria at 25°C (Frezza, Cipolat, &
209 Scorrano, 2007). Firstly, 2.1 mL of respiration buffer (composition previously described)
210 were added to the oxygraphic chamber supplemented with a mixture of glutamate (5 mM),
211 malate (2 mM) and succinate (5 mM). Then, mitochondria were added at a final concentration
212 of 0.2 mg/mL. Oxygen consumption rates were assessed without and with ADP (1 mM)
213 (basal and state 3, respectively). Then, CAT (5 µM) was added to block the oxygen
214 consumption linked to ATP synthesis. In order to evaluate the permeability of the
215 mitochondrial outer membrane, 10 µM of exogenous cytochrome c from equine heart were
216 added. At the end of the acquisition, CCCP was added to disrupt mitochondrial $\Delta\Psi_m$ and to
217 uncouple the respiratory chain, leading to an increase in oxygen consumption. The medium
218 was stirred continuously during measurement. Calibration using sodium dithionite was
219 performed to reach zero oxygen in the oxygraphic chamber.

220 Oxygen consumption rates were determined at each day of storage in the different
221 experimental conditions (basal, state 3, and CAT). As an index of mitochondrial coupling, the
222 respiratory control index (RCI) was calculated according to the following formula:

223 $$RCI = \frac{\text{state 3}}{\text{CAT}}$$

224 Where state 3 is the respiration rate during maximum ATP synthesis and CAT is the
225 respiration rate not linked to ATP synthesis. The integrity of the outer membrane was
226 evaluated by calculating the percentage of oxygen consumption not linked to ATP synthesis
227 stimulated following the addition of exogenous cytochrome c.

228 *2.7. Statistical analysis*

229 The statistical analysis and graphs were generated with SPSS 17 software. Each experiment
230 was performed at least in triplicate. Data are expressed as mean ± standard deviation.
231 Unpaired two-sample t-tests were used to express the significance of difference ($p < 0.05$)
232 between means, and Levene's test was used to determine the homogeneity of variance.

233 **3. Results**

234 *3.1 Ultrastructural analysis of* post mortem *fish muscle at different times of storage*

235 In order to study *post mortem* (PM) cell structural changes, the ultrastructure of gilthead sea
236 bream muscle tissue was observed by transmission electron microscopy (TEM) from Day 0 to
237 Day 6: Day 0 (6 h PM: Fig. 1a), Day 3 (72 h PM: Fig. 1b), Day 4 (96 h PM: Fig. 1c), Day 6
238 (144 h PM: Fig. 1d).

239 At Day 0, myofibrils were characterised by intact and well organised bands (I-bands and A-
240 bands) and lines (Z-lines and M-lines). The myofilaments of actin and myosin, which
241 constitute the sarcomere, were well defined and their alignment was parallel.

242 The disorganisation of the I-bands was observed from Day 3 of storage, and it was amplified
243 at Day 4 (Fig. 1.c). At Day 6, I-bands were barely identifiable (Fig. 1.d). The loss of density

244 of the Z-line was mainly observed at Day 6. The disruption of the parallel alignment of Z-
245 lines, M-lines and I-bands was observed from Day 3 (Fig. 1.b) and amplified at Day 6 (Fig.
246 1.d). From Day 3, the myofilaments of actin and myosin were no longer aligned and became
247 tight, with some gaps detectable.
248 Figures 1a to 1d also illustrate the effects of *post mortem* storage on mitochondrial structures.
249 The micrograph of gilthead sea bream muscle at Day 0 showed intact mitochondria with a
250 dense matrix. The cristae compartments were compact and well organised. For the majority of
251 the mitochondria, the double layer membranes were visible, with an intact and regular shape.
252 From Day 3, mitochondrial morphology began to change: mitochondria appeared swollen.
253 The shape of the membranes was discontinuous and in some places damaged. The cristae
254 were elongated, tubular, disorganised and had almost disappeared in some mitochondria. The
255 matrix had a more electron lucent appearance with the presence of a few dense granules (Fig.
256 1.b). The number of granules increased over time (few granules on Day 3, many granules on
257 Day 6 (Fig 1.d)). At Day 6, dense granules were located in nearly all mitochondria.
258 From a general point of view, gilthead sea bream fillet muscle cells underwent several major
259 structural changes from 3 days *post mortem* at +4°C. The mitochondria seemed to show
260 profound structural damage from the third day. The correlation between structural damage
261 and mitochondrial activity *post mortem* in fish fillet muscle was studied in the subsequent
262 experiments.

263 *3.2* Post mortem *assessment of mitochondrial function*

264 Here, we studied mitochondrial oxygen consumption in gilthead sea bream fillet muscle by
265 oxygraphy at different times of storage at +4°C (Fig. 2.a-e).
266 Figure 2 shows typical oxygraphic recordings of the changes in mitochondrial function from
267 Day 0 to Day 4 (a: Day 0; b: Day 1; c: Day 2; d: Day 3; e: Day 4). At Day 0 (Fig. 2a), basal
268 respiration (substrates only) reached 13.9 nmol O_2/min/mg proteins. Following ADP addition,

mitochondrial respiration was stimulated (39.95 nmol O_2/min/mg proteins), due to the consumption of the proton gradient by the ATP synthase. Addition of CAT inhibited the adenine nucleotides translocator and consequently ATP synthesis. As a consequence, oxygen consumption decreased to reach a new steady state of respiration not coupled to ATP synthesis (7 nmol O_2/min/mg proteins). The addition of cytochrome c, showing the integrity of the outer membrane of mitochondria by measuring the effect on respiration, demonstrated that the endogenous cytochrome c had no effect on respiration. The mitochondrial outer membrane was intact. Finally, the decoupling agent CCCP was added. The respiration rate strongly increased during a very short time, illustrating an increase of respiratory activity to maintain the disruption of $\Delta\Psi_m$ (Fig. 2a.b.c.d.). That was not the case for Day 4 (Fig. 2e).

The results for mitochondrial oxygen consumption at Day 0 were compared with mitochondrial oxygen consumption at Day 1 (Fig. 2.b), Day 2 (Fig. 2.c), Day 3 (Fig. 2.d), and Day 4 (Fig. 2.e).

From Day 0 (Fig. 2.a) to Day 3 (Fig. 2.d), the mean basal respiration rate was around 13.67 nmol O_2/min/mg proteins. From Day 4 (Fig. 2.e), the respiration rate increased to reach 17.75 nmol O_2/min/mg proteins. From Day 0 to Day 3 (Figs. 2.a-d), ADP, CAT and CCCP produced an effect on oxygen consumption. From Day 4 (Fig. 2.e), the effect of these compounds was very weak, which showed mitochondrial decoupling. From Day 0 (Fig. 2.a) to Day 4 (Fig. 2.e), the respiration rate at state 3 decreased gradually from 39.95 nmol O_2/min/mg proteins to 24.225 nmol O_2/min/mg proteins. From Day 0 (Fig. 2.a) to Day 3 (Fig. 2.d), the difference between the basal respiration rate and state 3 respiration rate was important. At Day 4 (Fig. 2.e), differences between the basal respiration rate (17.54 nmol O_2/min/mg proteins) and the state 3 respiration rate (24.22 nmol O_2/min/mg proteins) were very weak, demonstrating that ADP addition had barely effect.

293 Figure 3.a illustrates the repeatability of results from Figure 2, according to 3-5 independent
294 experiments. Changes in respiration (basal, state 3 and after CAT addition) are illustrated in
295 Figure 3a. From Day 0 to Day 3, no difference in basal respiration and a slight decrease of the
296 state 3 respiration rate were observed. By Day 4 (Fig. 3a), the basal respiratory rate had
297 increased by 45% (10.48 ± 3.10 nmol O_2/min/mg proteins to 15.93 ± 5.38 nmol O_2/min/mg
298 proteins, $p < 0.05$). At Day 4, an increase in the respiration rate after CAT addition was
299 observed (8.88 ± 2.36 nmol O_2/min/mg proteins to 15.66 ± 5.66 nmol O_2/min/mg proteins, p
300 < 0.05). At Day 4, mitochondria were not responding to ADP addition, indicating either
301 dysfunction of the ATP synthasome or increased permeability of the inner membrane to
302 protons.
303 The respiratory control index (RCI = state3/CAT) was calculated for each day (Fig. 3a). At
304 Day 0, RCI was 3.17 ± 0.71. RCI decreased from Day 0 to Day 4 to reach 1.30 ± 0.15,
305 illustrating a significant difference between Day 0 and Day 4 ($p < 0.05$).
306 External membrane integrity was measured by the addition of exogenous cytochrome c (Fig.
307 3.b). From Day 0 to Day 2, an elevation of the respiration rate was observed between 0.70 and
308 8%. An increase induced by cytochrome c was considered normal and acceptable when it is
309 between 5 and 15% (Kuznetsov, Veksler, Gellerich, Saks, Margreiter, & Kunz, 2008). From
310 Day 3, more than 30% stimulation of the respiratory rate was observed (38.5% ± 21.19 at Day
311 3 and 35% ± 19.06 at Day 4), illustrating that the outer membrane of mitochondria was
312 damaged.

313 *3.3* Post mortem *assessment of mitochondrial* $\Delta\Psi_m$
314 To further characterise changes in mitochondrial function *post mortem*, a qualitative
315 assessment of mitochondrial $\Delta\Psi_m$ was performed (Fig. 4). $\Delta\Psi_m$, being generated by the
316 electron transport chain, is correlated to mitochondrial function and integrity (Zorova,
317 Popkov, Plotnikov, Silachev, Pevzner, Jankauskas, et al., 2018). The potentiometric dye

318 Rh123 was used to qualitatively assess $\Delta\Psi_m$. Rh123 accumulates in the mitochondrial
319 compartment as a function of $\Delta\Psi_m$. The higher the potential, the more dye will enter the
320 matrix. Following accumulation and stacking of the dye within the matrix, its fluorescence is
321 quenched. Modulation of the electron transport chain activity by ADP, CAT or CCCP leads to
322 changes in $\Delta\Psi_m$ and consequent movement of the dye across the mitochondrial inner
323 membrane.
324 At Day 0 (Fig. 4.a), the addition of mitochondria to the buffer led to a strong fluorescence
325 intensity decrease (quenching). Then, when ADP was added (state 3), the Rh123 fluorescence
326 increased due to the release of the probe from the matrix in the surrounding buffer. ADP
327 addition led to a decrease in $\Delta\Psi_m$. In contrast, addition of CAT restored $\Delta\Psi_m$, and
328 consequently led to a decrease in fluorescence intensity. At the end of the experiment (Day 0;
329 Fig. 4.a), addition of CCCP disrupted $\Delta\Psi_m$ and led to a rapid increase in fluorescence. The
330 fluorescent signal did not reach the baseline value, indicating that part of the decreased
331 fluorescence following addition of mitochondria was not associated with the modulation of
332 $\Delta\Psi_m$.
333 From Day 0 to Day 4 (Fig. 4.a-e), the intensity of Rh123 fluorescence in the respiratory buffer
334 was evaluated in a same way. From Day 0 to Day 3 (Fig. 4.a-d), the addition of mitochondria
335 caused a fall in fluorescence of about 36% to 40%, which showed significant incorporation of
336 Rh123 and therefore high $\Delta\Psi_m$. At Day 4 (Fig. 4.e), the addition of mitochondria led to a
337 lower decrease in fluorescence (27%). From Day 0 to Day 3 (Fig. 4.a-d), addition of ADP, by
338 its decoupling action, decreased $\Delta\Psi_m$ and led to release of the probe (increase in
339 fluorescence). This action was less marked on Day 4 (Fig. 4.e). Conversely, by the blocking
340 action of the nucleotide transporters, CAT increased $\Delta\Psi_m$ and therefore the incorporation of
341 Rh123 into the mitochondria. This action was clearly identified from Day 0 to Day 3 (Fig.
342 4.a-d) and less marked from Day 4 (Fig. 4.e).

343 The action of CCCP (increased fluorescence due to Rh123 release) was related to the level of
344 probe incorporation, and was more visible at Days 0, 1, 2, and 3 (Fig. 4.a-d) than at Day 4
345 (Fig. 4.e). The results obtained at Day 4 revealed that $\Delta\Psi_m$ is disrupted.
346 In order to obtain an overall view of changes in $\Delta\Psi_m$ at different storage times *post mortem*,
347 the recorded fluorescence intensity was analysed at different states of respiration (Fig. 5). The
348 fluorescence associated with different states of respiration (basal/ADP/CAT) was normalised
349 by the fluorescence associated with CCCP treatment (as described in Materials and methods).
350 From Day 0 to Day 2, the effects of ADP and CAT on Rh123 fluorescence were significant.
351 From Day 3 to Day 4, neither ADP nor CAT affected Rh123 fluorescence, demonstrating
352 severe mitochondrial dysfunction.
353 From Day 3 to Day 4, the normalised Rh123 fluorescence was significantly higher for each
354 state of respiration in comparison with Days 0, 1, and 2. This increase reflected a lower intake
355 of Rh123 in the mitochondria, and consequently a fall in $\Delta\Psi_m$. On the basis of these results,
356 we can conclude that after 72 h of storage (Day 3) at +4°C, $\Delta\Psi_m$ started to decline and
357 became significantly disrupted after 96 hours (Day 4).

358 **4. Discussion**

359 The research of early markers of freshness is still a current challenge. This study focused, for
360 the first time, on mitochondria function as reliable indicator of fish freshness. Mitochondrial
361 activity was studied in fish skeletal muscle at different time points of *post mortem* storage at
362 +4°C in order to show structural and functional changes in *post mortem* mitochondria. The
363 structural changes were described based on electron microscopy images. A dual approach to
364 mitochondrial functionality (oxymetric approach and mitochondrial potential approach
365 ($\Delta\Psi_m$)) enabled us to better understand the alterations affecting the mitochondria in sea bream
366 fillet muscle. This research showed that mitochondria undergo profound *post mortem*
367 changes, which may be a relevant finding for assessment of food product freshness.

368 **Post mortem *structural changes in fish skeletal muscle***

369 Electron microscopy images were used to study the structural changes in mitochondria in fish
370 fillets stored *post mortem* at +4°C over 6 days. By choosing Days 3 and 4, we aimed to check
371 whether the observed mitochondrial activity changes were associated with major structural
372 changes. At Day 0 (6 hours *post mortem*), fish cell muscle retained its structural integrity. The
373 myofibril arrangement was conserved and well organised. No gaps between sarcomeres were
374 observable and collagen was still visible. These observations were consistent with those in
375 other studies, which described good preservation of muscle myofilaments in gilthead sea
376 bream fillet at Day 0 (María Dolores Ayala, et al., 2010; María Dolores Ayala, Santaella,
377 Martínez, Periago, Blanco, Vázquez, et al., 2011; Caballero, Betancor, Escrig, Montero, De
378 Los Monteros, Castro, et al., 2009). The majority of mitochondria were intact with non-
379 altered membranes and a network of compact and well organised cristae. Some authors who
380 have studied changes in myofilament structure in fish muscle have also been able to observe
381 changes in mitochondria (María Dolores Ayala, et al., 2010). For example, in gilthead sea
382 bream fillet (kept at +4°C), these authors observed swelling of some organelles, such as
383 mitochondria and sarcoplasmic reticulum 3 hours *post mortem*. Another study on sea bass,
384 carried out by the same authors, showed rapid changes in mitochondrial structure (with
385 swelling) 3 hours *post mortem* (Ma D Ayala, Albors, Blanco, Alcázar, Abellán, Zarzosa, et
386 al., 2005). Similarly, Roy, Ando, Itoh, and Tsukamasa (2012) described altered mitochondria
387 with swollen cristae in Pacific bluefin tuna muscle cells at Day 0. Studies specifically focused
388 on mammalian mitochondria showed good mitochondrial structure preservation several hours
389 *post mortem*. From a structural point of view, it appears that gilthead sea bream mitochondria
390 (like for mammalian mitochondria: (Barksdale, Perez-Costas, Gandy, Melendez-Ferro,
391 Roberts, & Bijur, 2010)) undergo few changes within a few hours of the animal's death. From
392 Day 3 to Day 6 (72 h – 144 h *post mortem*), several forms of structural damage in muscle

393 myofilaments were observed in gilthead sea bream fillet, with general disorganisation of
394 myofibril alignment, showing several gaps. The same observations were reported from Day 5
395 in gilthead sea bream muscle, such as alterations of sarcomeres at the I-band level, alteration
396 of actin filaments, and disruption of Z-lines (María Dolores Ayala, et al., 2011).
397 Mitochondria were swollen with disrupted membranes and dense granules in the
398 mitochondrial matrix. Dense granules were also observed (María Dolores Ayala, et al., 2010)
399 on gilthead sea bream mitochondria from 5 days *post mortem*. These granules have also been
400 observed *post mortem* in mammalian mitochondria (Kuypers & Roomans, 1980). Importantly,
401 an explanation was offered for the appearance of dense granules in mitochondria (Wolf,
402 Mutsafi, Dadosh, Ilani, Lansky, Horowitz, et al., 2017). These authors showed that the
403 granules resulted from the accumulation and precipitation of calcium in the mitochondrial
404 matrix. During cell death processes, calcium homeostasis is profoundly disturbed, leading to
405 massive calcium entry into the mitochondria (Dong, Saikumar, Weinberg, & Venkatachalam,
406 2006). This flux initially caused swelling of the organelles and then precipitation of calcium
407 as insoluble phosphate and hydroxyapatite, which participated in mitochondrial damage and
408 cell death (Dong, Saikumar, Weinberg, & Venkatachalam, 2006). The calcium aggregation in
409 ischaemic conditions described by these authors could be similar to that found *post mortem* in
410 muscle cells, which were also deprived of oxygen.

411 *Mitochondrial activity: an early fish freshness indicator*

412 In the second part of our study, we focused on mitochondrial activity *post mortem* in fish
413 muscle cells at different storage time points at +4°C: Day 0 (6 h), Day 1 (24 h), Day 2 (48 h),
414 Day 3 (72 h), and Day 4 (96 h). Two approaches based on oxygraphy and fluorescence
415 enabled us to investigate mitochondrial activity.
416 Mitochondria maintained significant respiratory activity for the first 3 days of storage (Day 0
417 to Day 3). From Day 4, respiratory activity declined significantly (96 hours *post mortem*):

418 RCI (1.30 ± 0.15) was significantly lower than at Day 0 (3.17 ± 0.71). RCI is a useful
419 measure to assess mitochondrial function in isolated mitochondria, and its decrease is
420 associated with mitochondrial dysfunction (Brand & Nicholls, 2011). This mitochondrial
421 dysfunction resulted from electron transport chain alteration, and this activity can be explored
422 with different substrates (ADP, CAT, cytochrome C, and CCCP). On the fourth day (Day 4),
423 decoupling agents such as CCCP and ADP had no action on mitochondrial respiration (no
424 increase in respiratory activity), showing the inability of respiratory chains to adapt to the loss
425 of mitochondrial potential (via ADP or CCCP addition). Mitochondrial decoupling at Day 4
426 could be due to mitochondrial membrane permeabilisation. Alteration of the mitochondrial
427 outer membrane was confirmed by the activating effect of exogenous cytochrome c on
428 respiration activity (30% at Day 4).
429 The fluorescent probe Rh123 was used to evaluate the $\Delta\Psi_m$ of isolated mitochondria. By
430 comparing findings with oxygraphic results, we can clearly observe the uncoupling action of
431 ADP and CCCP on mitochondria isolated from sea bream fillets stored at +4°C (Day 0, Day
432 1, and Day 2). ADP and CCCP led to dissipation of mitochondrial potential, which decreased
433 the uptake of the probe and thus increased the overall fluorescence in the surrounding buffer.
434 From Day 3, ADP and CCCP additions had no significant effects on Rh123 fluorescence
435 intensity, indicating mitochondrial decoupling. In addition, the intensity of Rh123
436 fluorescence increased from Day 3 for all states of respiration. This increase was associated
437 with a decrease in Rh123 quenching. The high values for standard deviations obtained at Day
438 3, representative of eight independent experiments, highlighted the marked heterogeneity of
439 the results at this precise time compared to Day 4. Overall, the results obtained with the
440 Rh123 fluorescent probe demonstrated that $\Delta\Psi_m$ was strongly and significantly disrupted
441 from Day 4. This disruption was correlated to the decline in mitochondrial activity, and
442 consequently to cell health and mitochondrial membrane integrity (Zorova, et al., 2018).

443 The two approaches (oxygraphic and fluorescence) coincided well and showed that isolated
444 mitochondria of sea bream fillets stored at +4°C retained activity 2 to 3 days *post mortem*.
445 From Day 3/Day 4, mitochondrial respiratory activity and $\Delta\Psi_m$ strongly decreased. On the
446 basis of the concept developed by Cheah and Cheah (1971), the "critical storage time" was
447 between 72 hours (Day 3) and 96 hours (Day 4) for the *Sparus aurata* model stored on ice at
448 +4°C. Maintenance of mitochondrial activity has been demonstrated in other studies in ox
449 neck muscle (Cheah & Cheah, 1971, 1974) and in mouse and human brain tissue (Barksdale,
450 Perez-Costas, Gandy, Melendez-Ferro, Roberts, & Bijur, 2010).
451 In stress conditions of anoxia present after death, calcium homeostasis is disrupted and
452 calcium levels increase in the sarcoplasm. Mitochondria have the ability to maintain their
453 activity *post mortem*. This maintenance occurs because mitochondrial ATP synthase can run
454 in reverse, hydrolysing ATP generated by glycolysis in order to maintain $\Delta\Psi_m$ (St-Pierre,
455 Brand, & Boutilier, 2000). Sarcoplasmic calcium enters mitochondria through the maintained
456 $\Delta\Psi_m$. From Day 3/Day 4, marked calcium accumulation in mitochondria was found and
457 appeared in the form of dense granules by electron microscopy. Mitochondrial calcium
458 overload developed, leading to $\Delta\Psi_m$ disruption and mitochondrial membrane permeabilisation
459 (Dong, Saikumar, Weinberg, & Venkatachalam, 2006). Membrane permeabilisation may be
460 associated with the formation of mitochondrial permeability transition pores, leading to the
461 release of cell death-inducing factors, cytochrome c, and huge amounts of calcium in the
462 sarcoplasm. This release probably plays a role in integrating death signals and may participate
463 in proteolytic enzyme activation (via the release of cytochrome c and mitochondrial calpain
464 activation) (Boudida, Becila, Gagaoua, Boudjellal, Sentandreu, & Ouali, 2015; Smith &
465 Schnellmann, 2012).
466 Day 4 is a crucial storage time point in gilthead sea bream muscle cells, and is the starting
467 point of marked cell alteration. From Day 4, it has been reported that insoluble collagen

468 decreased strongly, leading to a loss of firmness and an increase in the water-holding capacity
469 (Suárez, Abad, Ruiz-Cara, Estrada, & García-Gallego, 2005). At Day 4, the molecule
470 dystrophin, which provides a link between cytoskeletal actin and the extracellular matrix,
471 almost disappeared, while actin and desmin were detected in fish muscle at early stages of
472 alteration *post mortem* (14 days). Loss of dystrophin is correlated to detachment myofibres
473 and myocommata, and a reduction in flesh hardness (Caballero, et al., 2009). From Day 4,
474 free LDH activity released from sea bream muscle strongly increased, demonstrating an
475 increase of fish autolysis after 4 days of storage at +4°C (Diop, Watier, Masson, Diouf,
476 Amara, Grard, et al., 2016).
477 In future studies, it would be interesting to assess whether mitochondrial activity is
478 maintained for a longer period of time in other experimental conditions, such as a storage
479 temperature of +0°C/+2°C, the use of natural additives, or modified atmosphere packaging.

480 **5. Conclusion**

481 The mitochondrial structural changes (swelling, membrane and cristae alteration, and
482 accumulation of dense granules) were correlated with an increase in permeability (sensitivity
483 to cytochrome c), $\Delta\Psi_m$ disruption, and a decrease in respiratory activity. The mitochondria of
484 sea bream fillets stored at +4°C maintained significant respiratory activity for the first three
485 days of storage. Therefore, mitochondria could be useful targets for evaluating the freshness
486 of seafood, and the starting point for the development of a fish freshness kit concerning the
487 first stages of spoilage. It would be very interesting to determine whether these structural and
488 physiological mitochondrial changes in a fresh seafood product (such as fish fillets) have an
489 influence on perceptions and the health of consumers.

Acknowledgements

Jérôme Cléach would like to thank the *Pôle Métropolitain de la Côte d'Opale* council and *PFI Nouvelles Vagues* for their financial support of his PhD studies.

Funding

This study was funded by the French government and the Hauts-de-France region in the framework of the CPER 2014-2020 MARCO project. This research was also funded by FranceAgrimer in the framework of the Altfish project.

References

Ayala, M. D., Abdel, I., Santaella, M., Martínez, C., Periago, M. J., Gil, F., Blanco, A., & Albors, O. L. (2010). Muscle tissue structural changes and texture development in sea bream, *Sparus aurata* L., during post-mortem storage. *LWT-Food Sci. Technol., 43*(3), 465-475.

Ayala, M. D., Albors, O. L., Blanco, A., Alcázar, A. G., Abellán, E., Zarzosa, G. R., & Gil, F. (2005). Structural and ultrastructural changes on muscle tissue of sea bass, *Dicentrarchus labrax* L., after cooking and freezing. *Aquaculture, 250*(1-2), 215-231.

Ayala, M. D., Santaella, M., Martínez, C., Periago, M. J., Blanco, A., Vázquez, J. M., & Albors, O. L. (2011). Muscle tissue structure and flesh texture in gilthead sea bream, *Sparus aurata* L., fillets preserved by refrigeration and by vacuum packaging. *LWT-Food Sci. Technol., 44*(4), 1098-1106.

Barksdale, K. A., Perez-Costas, E., Gandy, J. C., Melendez-Ferro, M., Roberts, R. C., & Bijur, G. N. (2010). Mitochondrial viability in mouse and human postmortem brain. *FASEB J., 24*(9), 3590-3599.

Blier, P. U., & Guderley, H. E. (1993). Mitochondrial activity in rainbow trout red muscle: the effect of temperature on the ADP-dependence of ATP synthesis. *J. Exp. Biol., 176*(1), 145-158.

Boudida, Y., Becila, S., Gagaoua, M., Boudjellal, A., Sentandreu, M., & Ouali, A. (2015). Muscle to meat conversion in common carp (*cyprinus carpio*): new insights involving apoptosis. In *61th. International Congress of Meat Science and Technology (ICoMST). 2015; 61. International Congress of Meat Science and Technology (ICoMST), Clermont-Ferrand, FRA, 2015-08-23-2015-08-28, 162-162*): INRA.

Brand, M. D., & Nicholls, D. G. (2011). Assessing mitochondrial dysfunction in cells. *Biochem. J., 435*(2), 297-312.

Caballero, M., Betancor, M., Escrig, J., Montero, D., De Los Monteros, A. E., Castro, P., Ginés, R., & Izquierdo, M. (2009). Post mortem changes produced in the muscle of sea bream (*Sparus aurata*) during ice storage. *Aquaculture, 291*(3-4), 210-216.

Cambier, S., Benard, G., Mesmer-Dudons, N., Gonzalez, P., Rossignol, R., Brethes, D., & Bourdineaud, J.-P. (2009). At environmental doses, dietary methylmercury inhibits mitochondrial energy metabolism in skeletal muscles of the zebra fish (*Danio rerio*). *Int. J. Biochem. Cell Biol., 41*(4), 791-799.

529 Castro, P., Padrón, J. C. P., Cansino, M. J. C., Velázquez, E. S., & Larriva, R. M. D. (2006).
530 Total volatile base nitrogen and its use to assess freshness in European sea bass stored
531 in ice. *Food Control, 17*(4), 245-248.
532 Cheah, K., & Cheah, A. (1971). Post-mortem changes in structure and function of ox muscle
533 mitochondria. 1. Electron microscopic and polarographic investigations. *J. Bioenerg.,*
534 *2*(2), 85-92.
535 Cheah, K., & Cheah, A. (1974). Properties of mitochondria from ox neck muscle after storage
536 in situ. *Int. J. Biochem., 5*(9-10), 753-760.
537 Cheng, J. H., Sun, D. W., Han, Z., & Zeng, X. A. (2014). Texture and structure measurements
538 and analyses for evaluation of fish and fillet freshness quality: a review. *Compr. Rev.*
539 *Food Sci. Food Saf., 13*(1), 52-61.
540 Delbarre-Ladrat, C., Chéret, R., Taylor, R., & Verrez-Bagnis, V. (2006). Trends in
541 postmortem aging in fish: understanding of proteolysis and disorganization of the
542 myofibrillar structure. *Crit. Rev. Food Sci. Nutr., 46*(5), 409-421.
543 Diop, M., Watier, D., Masson, P.-Y., Diouf, A., Amara, R., Grard, T., & Lencel, P. (2016).
544 Assessment of freshness and freeze-thawing of sea bream fillets (*Sparus aurata*) by a
545 cytosolic enzyme: Lactate dehydrogenase. *Food Chem., 210*, 428-434.
546 Dong, Z., Saikumar, P., Weinberg, J. M., & Venkatachalam, M. A. (2006). Calcium in cell
547 injury and death. *Annu. Rev. Pathol. Mech. Dis., 1*, 405-434.
548 Emaus, R. K., Grunwald, R., & Lemasters, J. J. (1986). Rhodamine 123 as a probe of
549 transmembrane potential in isolated rat-liver mitochondria: spectral and metabolic
550 properties. *Biochim. Biophys. Acta, Bioenerg., 850*(3), 436-448.
551 Frezza, C., Cipolat, S., & Scorrano, L. (2007). Organelle isolation: functional mitochondria
552 from mouse liver, muscle and cultured filroblasts. *Nat. Protoc., 2*(2), 287.
553 Hilton, Z., Clements, K. D., & Hickey, A. J. (2010). Temperature sensitivity of cardiac
554 mitochondria in intertidal and subtidal triplefin fishes. *J. Comp. Physiol., B, 180*(7),
555 979-990.
556 Kuypers, G. A., & Roomans, G. M. (1980). Post-mortem elemental redistribution in rat
557 studied by X-ray microanalysis and electron microscopy. *Histochemistry, 69*(2), 145-
558 156.
559 Kuznetsov, A. V., Veksler, V., Gellerich, F. N., Saks, V., Margreiter, R., & Kunz, W. S.
560 (2008). Analysis of mitochondrial function in situ in permeabilized muscle fibers,
561 tissues and cells. *Nature protocols, 3*(6), 965.
562 Lionetti, L., Mollica, M. P., Donizzetti, I., Gifuni, G., Sica, R., Pignalosa, A., Cavaliere, G.,
563 Gaita, M., De Filippo, C., & Zorzano, A. (2014). High-lard and high-fish-oil diets
564 differ in their effects on function and dynamic behaviour of rat hepatic mitochondria.
565 *PloS one, 9*(3), e92753.
566 Mendes, R. (2018). Technological processing of fresh gilthead seabream (*Sparus aurata*): A
567 review of quality changes. *Food Rev. Int.*, 1-34.
568 Michalec, F.-G., Holzner, M., Barras, A., Lacoste, A.-S., Brunet, L., Lee, J.-S., Slomianny,
569 C., Boukherroub, R., & Souissi, S. (2017). Short-term exposure to gold nanoparticle
570 suspension impairs swimming behavior in a widespread calanoid copepod. *Environ.*
571 *Pollut., 228*, 102-110.
572 Oehlenschläger, J., & Sörensen, N. (1997). Criteria of fish freshness and quality aspects. In
573 *The Final Meeting of the Concerted Action-Evaluation of Fish Freshness-1997*, (pp.
574 30-35).
575 Olafsdottir, G., Martinsdóttir, E., Oehlenschläger, J., Dalgaard, P., Jensen, B., Undeland, I.,
576 Mackie, I., Henehan, G., Nielsen, J., & Nilsen, H. (1997). Methods to evaluate fish
577 freshness in research and industry. *Trends Food Sci. Technol., 8*(8), 258-265.

578 Olafsdottir, G., Nesvadba, P., Di Natale, C., Careche, M., Oehlenschläger, J., Tryggvadóttir,
579 S., Schubring, R., Kroeger, M., Heia, K., Esaiassen, M., Macagnano, A., & Jørgensen,
580 B. (2004). Multisensor for fish quality determination. *Trends Food Sci. Technol.,*
581 *15*(2), 86-93.
582 Olafsdottir, G., Nesvadba, P., Di Natale, C., Careche, M., Oehlenschläger, J., Tryggvadottir,
583 S. V., Schubring, R., Kroeger, M., Heia, K., & Esaiassen, M. (2004). Multisensor for
584 fish quality determination. *Trends in Food Science & Technology, 15*(2), 86-93.
585 Parlapani, F. F., Mallouchos, A., Haroutounian, S. A., & Boziaris, I. S. (2014).
586 Microbiological spoilage and investigation of volatile profile during storage of sea
587 bream fillets under various conditions. *Int. J. Food Microbiol., 189*, 153-163.
588 Parsons, M. J., & Green, D. R. (2010). Mitochondria in cell death. *Essays Biochem., 47*, 99-
589 114.
590 Pasdois, P., Parker, J. E., Griffiths, E. J., & Halestrap, A. P. (2011). The role of oxidized
591 cytochrome c in regulating mitochondrial reactive oxygen species production and its
592 perturbation in ischaemia. *Biochemical Journal, 436*(2), 493-505.
593 Roy, B. C., Ando, M., Itoh, T., & Tsukamasa, Y. (2012). Structural and ultrastructural
594 changes of full-cycle cultured Pacific bluefin tuna (*Thunnus orientalis*) muscle slices
595 during chilled storage. *J. Sci. Food Agric., 92*(8), 1755-1764.
596 Smith, M. A., & Schnellmann, R. G. (2012). Calpains, mitochondria, and apoptosis.
597 *Cardiovasc. Res., 96*(1), 32-37.
598 Soares, S. S., Gutierrez-Merino, C., & Aureliano, M. (2007). Mitochondria as a target for
599 decavanadate toxicity in *Sparus aurata* heart. *Aquat. Toxicol., 83*(1), 1-9.
600 St-Pierre, J., Brand, M. D., & Boutilier, R. G. (2000). Mitochondria as ATP consumers:
601 cellular treason in anoxia. *Proc. Natl. Acad. Sci. U. S. A., 97*(15), 8670-8674.
602 Suárez, M. D., Abad, M., Ruiz-Cara, T., Estrada, J. D., & García-Gallego, M. (2005).
603 Changes in muscle collagen content during *post mortem* storage of farmed sea bream
604 (*Sparus aurata*): influence on textural properties. *Aquacult. Int., 13*(4), 315-325.
605 Tang, J., Faustman, C., Hoagland, T. A., Mancini, R. A., Seyfert, M., & Hunt, M. C. (2005).
606 Postmortem oxygen consumption by mitochondria and its effects on myoglobin form
607 and stability. *J. Agric. Food Chem., 53*(4), 1223-1230.
608 Taylor, R., Fjaera, S., & Skjervold, P. (2002). Salmon fillet texture is determined by
609 myofiber-myofiber and myofiber-myocommata attachment. *J. Food Sci., 67*(6), 2067-
610 2071.
611 Van den Thillart, G., & Modderkolk, J. (1978). The effect of acclimation temperature on the
612 activation energies of state III respiration and on the unsaturation of membrane lipids
613 of goldfish mitochondria. *Biochim. Biophys. Acta, Biomembr., 510*(1), 38-51.
614 Wolf, S. G., Mutsafi, Y., Dadosh, T., Ilani, T., Lansky, Z., Horowitz, B., Rubin, S., Elbaum,
615 M., & Fass, D. (2017). 3D visualization of mitochondrial solid-phase calcium stores in
616 whole cells. *Elife, 6*.
617 Zorova, L. D., Popkov, V. A., Plotnikov, E. Y., Silachev, D. N., Pevzner, I. B., Jankauskas, S.
618 S., Babenko, V. A., Zorov, S. D., Balakireva, A. V., Juhaszova, M., Sollott, S. J., &
619 Zorov, D. B. (2018). Mitochondrial membrane potential. *Anal. Biochem., 552*, 50-59.

620

621 **Figure captions**

622 **Figure 1:** Longitudinal sections of gilthead sea bream muscle at different *post mortem* times:
623 6 h *post mortem* (Day 0) (a), 72 h (Day 3) (b), 96 h (Day 4) (c), and 144 h (Day 6) (d). A: A
624 band; col: collagen; dg: dense granules; H: H zone; I: I band; M: M line; mit: mitochondria;
625 sar: sarcoplasm; sr: sarcoplasmic reticulum; Tr: triad; Z: Z line. Bars: a, b, c, d: 500 nm.

626 **Figure 2:** *Post mortem* assessment of respiratory activity of gilthead sea bream isolated
627 mitochondria by oxygraphy
628 Oxygraph traces and their first derivate (dotted line) are represented at different storage times:
629 Day 0 (a), Day 1 (b), Day 2 (c), Day 3 (d), and Day 4 (e). After the addition of mitochondria
630 (mito.) (0.2 mg/mL), the molecules ADP (2 mM), CAT (5 µM), cytochrome c (Cyt. C) (10
631 µM) and CCCP (2 µM) were added to the incubation chamber. These graphs are
632 representative of one experiment.

633 **Figure 3:** Evaluation of mitochondrial intactness parameters
634 RCI, respiration rates (a) and stimulation of respiration by cytochrome c (b) at different *post*
635 *mortem* intervals. The mitochondria were isolated from gilthead sea bream muscle at different
636 storage times: Day 0, Day 1, Day 2, Day 3 and Day 4. White circles denote values that are
637 significantly different from values recorded at Day 0, Day 1, or Day 2. Daggers denote values
638 that are significantly different. The t-test was performed using the SPSS Statistic 17
639 programme; ($p < 0.05$; N=3-5).

640 **Figure 4:** *Post mortem* assessment of the mitochondrial membrane potential of gilthead sea
641 bream isolated mitochondria by fluorimetry (Safas).
642 Rhodamine 123 fluorescence traces of isolated mitochondria are represented at different
643 storage times: Day 0 (a), Day 1 (b), Day 2 (c), Day 3 (d), and Day 4 (e). After the addition of

644 mitochondria (Mito.) (0.2 mg/mL), the molecules ADP (2 mM), CAT (5 µM) and CCCP (2
645 µM) were added to a 3 mL cuvette. These graphs are representative of one experiment.

646 **Figure 5:** Summary graphs of Rh123 fluorescence levels at different states of respiration
647 normalised to CCCP at different storage times. The different storage times were: Day 0, Day
648 1, Day 2, Day 3, and Day 4. Asterisks denote values that are significantly different at different
649 storage times. The t-test was performed using the SPSS Statistic 17 programme; ($p < 0.05$;
650 N=4-8).

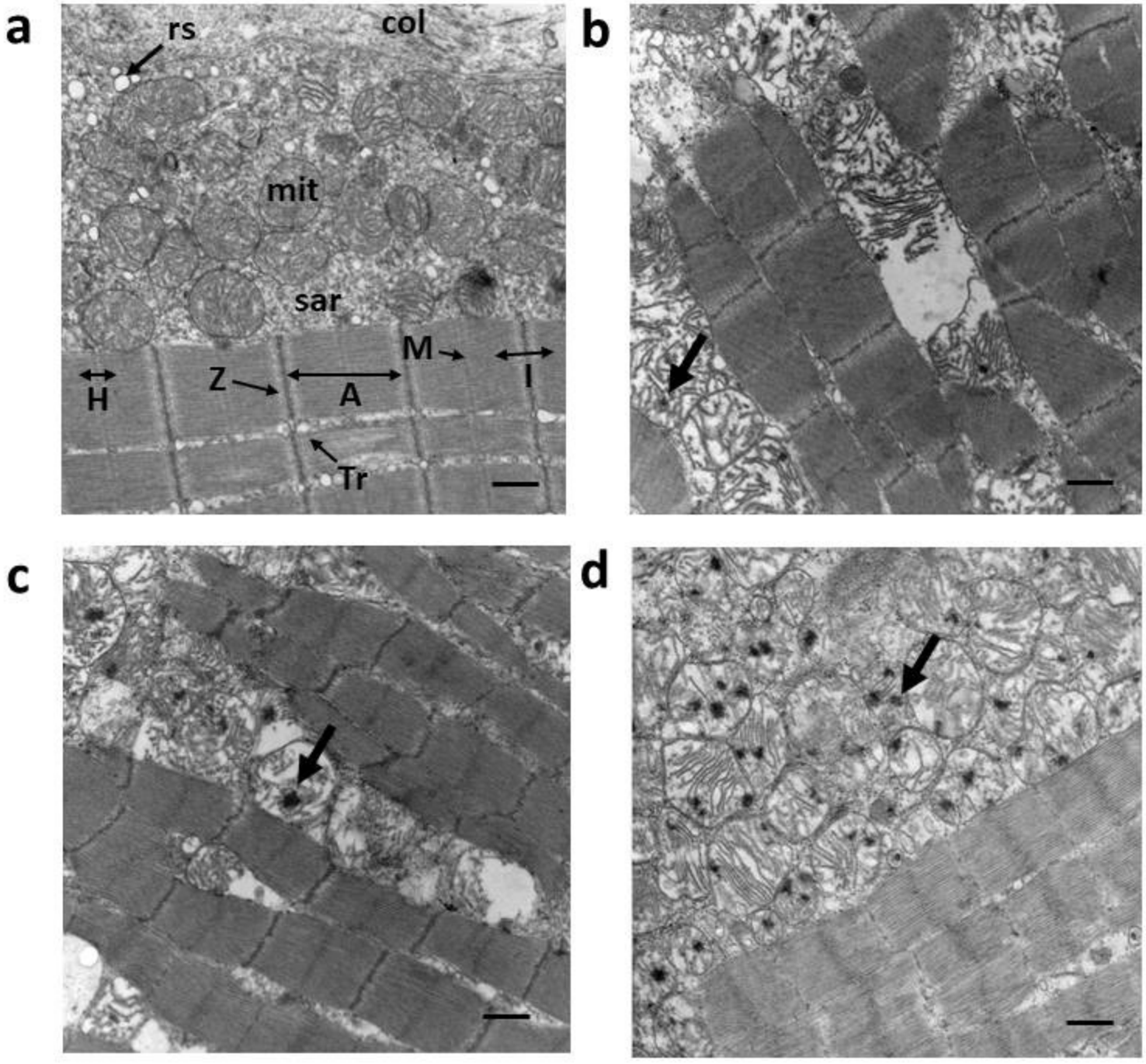
a
rs
col
mit
sar
M
Z
A
I
H
Tr
b
c
d

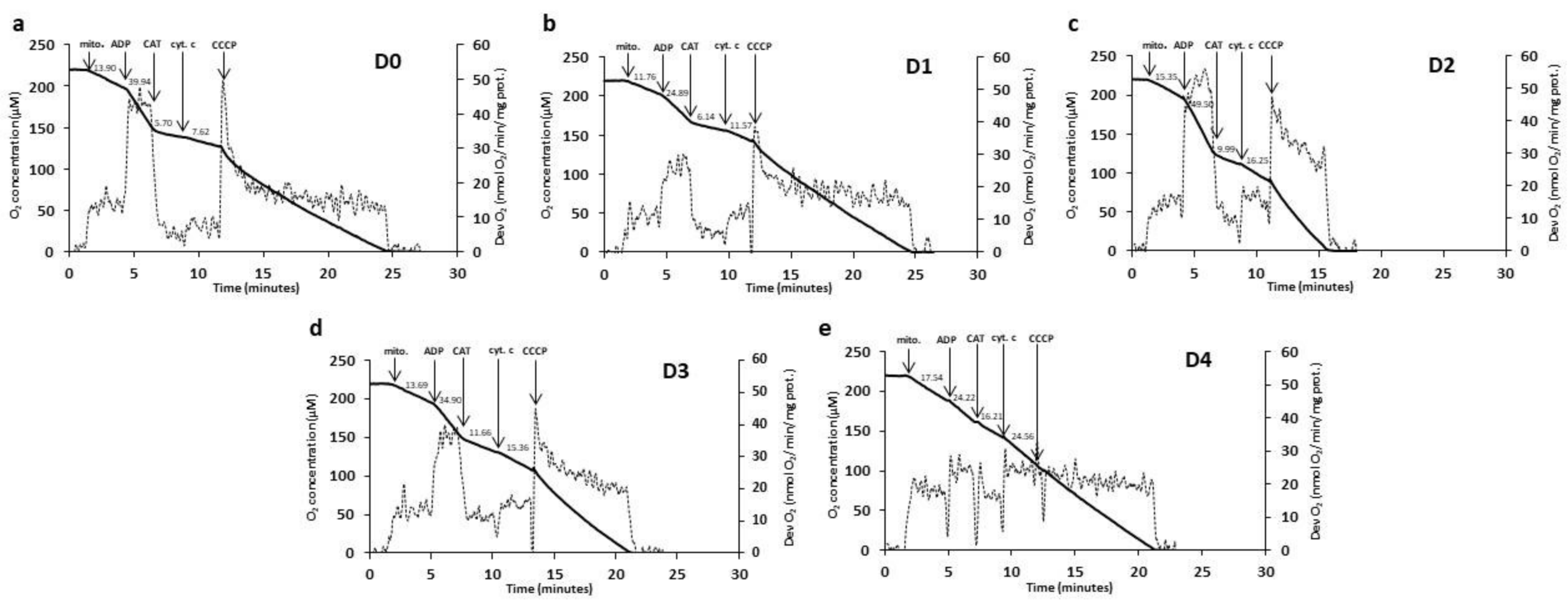
a
D0
mito.
ADP
CAT
cyt. c
CCCP
13.90
39.94
5.70
7.62
b
D1
11.76
24.89
6.14
11.57
c
D2
15.35
49.56
9.99
16.25
d
D3
13.69
34.90
11.66
15.36
e
D4
17.54
24.22
16.21
24.56
O2 concentration (µM)
Dev O2 (nmol O2/ min/ mg prot.)
Time (minutes)

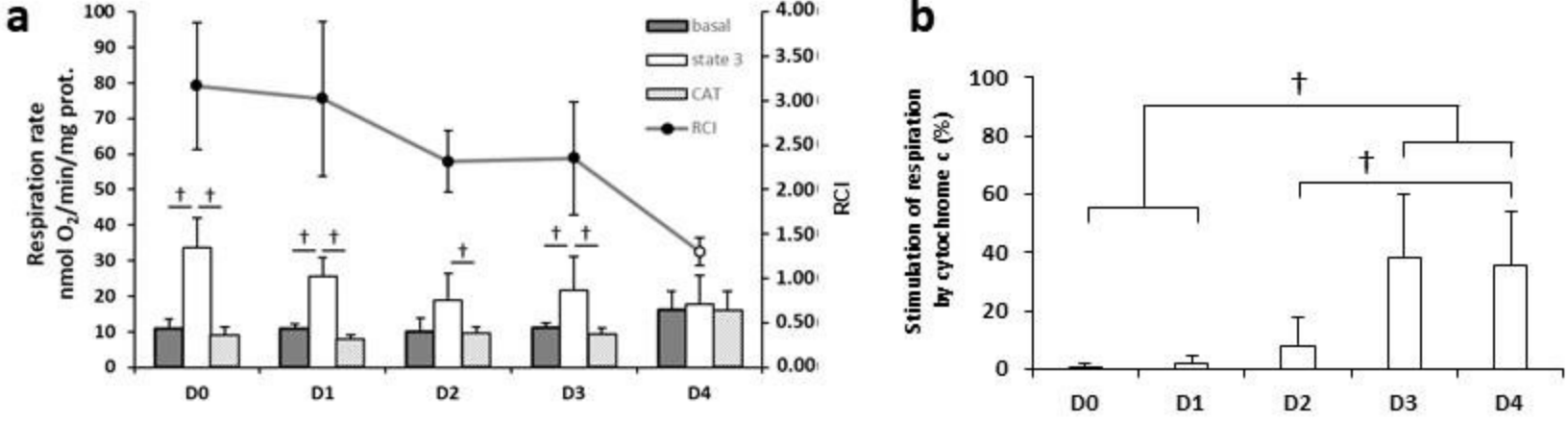
a
Respiration rate
nmol O2/min/mg prot.
RCI
basal
state 3
CAT
RCI
D0
D1
D2
D3
D4
b
Stimulation of respiration
by cytochrome c (%)
D0
D1
D2
D3
D4

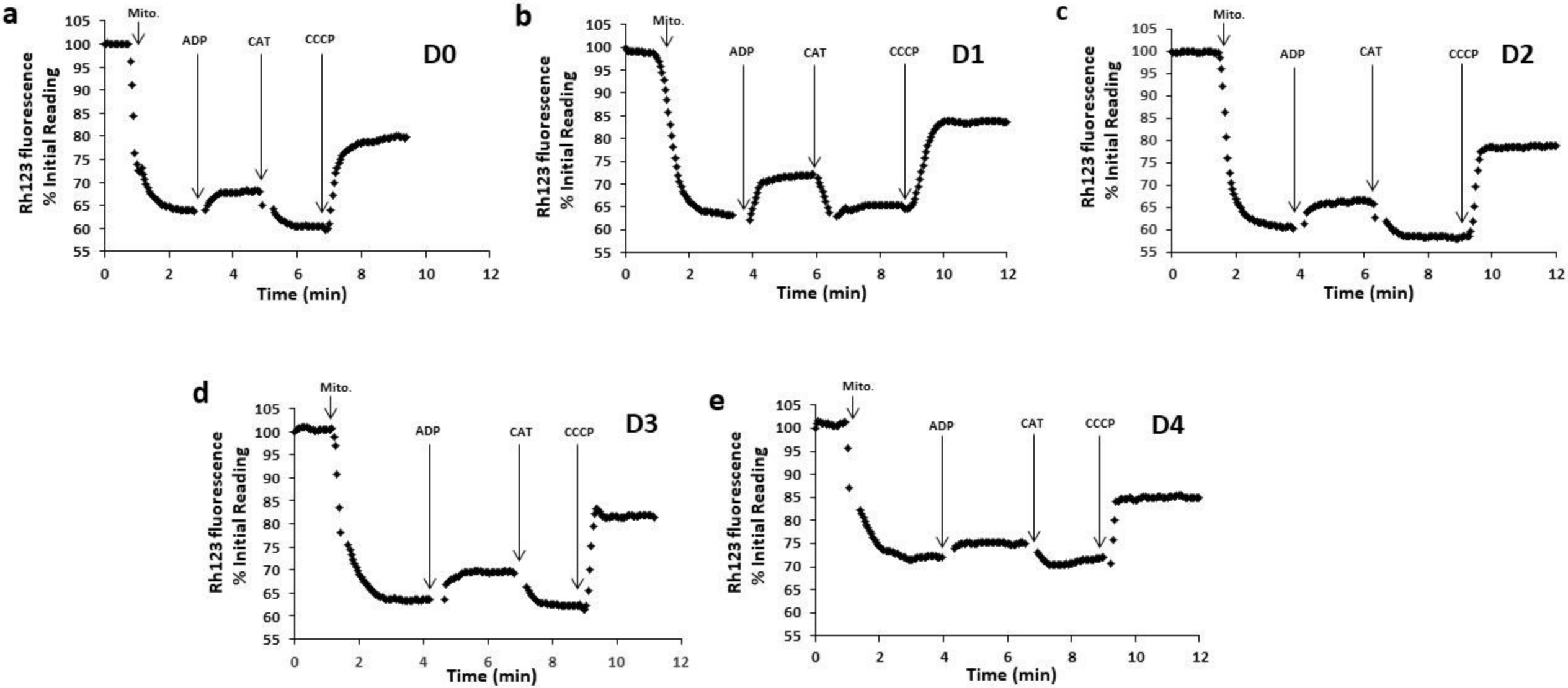
a
Mito.
ADP
CAT
CCCP
D0
Rh123 fluorescence
% Initial Reading
Time (min)
b
D1
c
D2
d
D3
e
D4

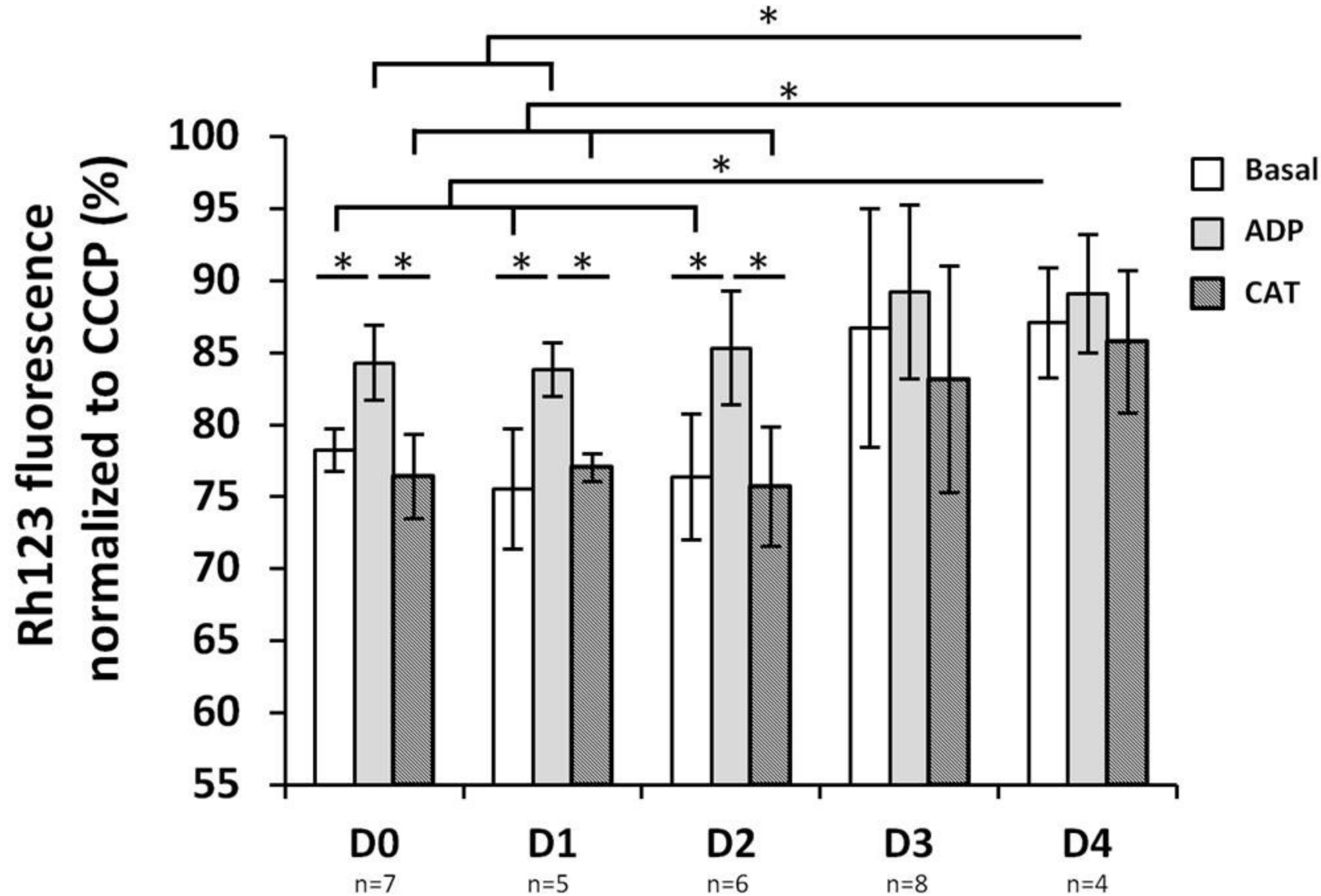
Rh123 fluorescence normalized to CCCP (%)
100
95
90
85
80
75
70
65
60
55
Basal
ADP
CAT
*
D0
n=7
D1
n=5
D2
n=6
D3
n=8
D4
n=4